# DESIGN AND IMPLEMENTATION OF AN IMAGE PROCESSING ALGORITHM FOR VELOCIMETRY SYSTEMS

PROJETO E IMPLEMENTAÇÃO DE UM ALGORITMO DE PROCESSAMENTO DE IMAGENS PARA SISTEMAS DE VELOCIMETRIA

**Roger Pizzato Nunes**

Universidade Federal do Rio Grande do Sul
Instituto de Física – Departamento de Física
Av. Bento Gonçalves, 9500, Caixa Postal 15051
91501-970 – Porto Alegre, RS, Brasil
E-mail: rogerpn@if.ufrgs.br

## ABSTRACT

The fluid dynamics presents a complex behavior and in certain regimes it has not been theoretically understood by the physics laws yet. For this reason, the experimental techniques of flow visualization have been used since the 70's with the first methods introduced in laser applications like LDV (Laser Doppler Velocimetry). In these last ten years, due to the digital CCD camera improvements, the development of frame grabbers and microcomputers with better processing performance and large memory, image processing techniques have been applied to investigate fluid dynamics. However, the scientific works in this field of velocimetry through image processing have been always focused in the physical basis behind the measurement, in the improvements or developments of specific algorithms, and in the use of different equipments for instrumentation, not considering the engineering aspects involved in the methodology for the conception and the design of the entire Velocimetry System. In this way, this work presents the design and the implementation of an image processing algorithm for the measurement of the two-dimensional velocity field of fluid flows. This image processing algorithm is a part of a whole Velocimetry System developed by us and that has been successfully applied to different physical systems as our recent publications shown.
**Keywords:** flow visualization, signal processing, electro-electronic instrumentation, and Velocimetry System.

## RESUMO

A dinâmica de fluidos apresenta um comportamento complexo e em certo regimes ainda não é adequadamente compreendida pelas leis da Física. Por esta razão, técnicas experimentais de visualização de escoamentos têm sido utilizadas desde a década de 70, com os primeiros métodos introduzidos em aplicações envolvendo LASER tais como LDV (Laser Doppler Velocimetry). Nestes últimos 10 anos, devido ao aperfeiçoamento das câmeras digitais CCD, ao desenvolvimento de placas de captura e de microcomputadores com melhor desempenho e maior memória, técnicas de processamento de imagens têm sido aplicadas na investigação da dinâmica de fluidos. Contudo, trabalhos científicos nesta área de Velocimetria por processamento de imagens têm focado usualmente o embasamento físico deste tipo de medida, o aperfeiçoamento ou desenvolvimento de algoritmos específicos e a utilização de diferentes equipamentos para instrumentação, não considerando os aspectos de engenharia envolvidos na metodologia de concepção e de projeto do Sistema de Velocimetria como um todo. Neste sentido, este trabalho apresenta o projeto e a implementação de um algoritmo de processamento de imagens para a medição de campos bidimensionais de velocidade de escoamentos. Este algoritmo de processamento de imagens corresponde à uma parte de um Sistema de Velocimetria desenvolvido pelo autor e que tem sido aplicado em diferentes sistemas físicos com sucesso, conforme mostram recentes publicações.
**Palavras-chave**: visualização de escoamentos, processamento de sinais, instrumentação eletroeletrônica e Sistemas de Velocimetria.

## 1 – INTRODUCTION

In the macroscopic view, the mathematical description of the state of a moving fluid is effected by means of functions which give the distribution of the fluid velocity $\mathbf{v}(\mathbf{r}, t)$ and of any two thermodynamic quantities pertaining to the fluid like the pressure and density, forming a hydrodynamic and thermal coupled problem. If these five quantities are determined, namely the 3 components of the velocity field $\mathbf{v}$, the pressure, and the temperature, the dynamics of the fluid is completely described. For each one of these quantities there is a nonlinear partial differential equation that has to be solved for a specific boundary condition [1].

The paragraph above has been intended to contextualize the complexity of the physical systems in the area of fluid mechanics. As a consequence of this complexity, the turbulence is a problem that has not been understood and theoretically described by the classical physics yet [2]. Thus, nowadays, the experimental results

still play an important role to achieve necessary empirical relations in projects of engineering in the areas of aerodynamics [3], turbomachinery [4], biomedical [5], metallurgy [6], and others. In the academic scope, these experimental results are still used for the development and the validation of models that describe the mechanisms involved in the turbulence phenomenon [7][8]. With the validated models, it is possible to understand better the physical mechanisms that are already unknown in the area of fluid dynamics.

Considering an incompressible flow and the regimes where the thermodynamic effects can be neglected, the instantaneous velocity field of a fluid flow is the more important and fundamental physical quantity of fluid dynamics. With the instantaneous velocity field, it is possible to compute spatial fluid flow quantities like vorticity and circulation, and time fluid flow quantities like the intensity of turbulence, among others. These quantities completely determine the characterization of the fluid flow under analysis [9].

In the last years, many experimental techniques had been developed to measure the velocity of a fluid flow [10]. However, the evolution of the image sensors like the CCD (Charged Coupled Device) allowed that velocimetry techniques through image processing have been developed [11]. With these techniques, it is possible to obtain quantitative and qualitative information of the transient or of the steady state of the fluid flow in analysis. The main profit of these techniques in relation to the traditional ones is the possibility for a given time $t = t_o$ to measure a whole velocity field $\mathbf{v}(\mathbf{r}, \mathrm{t_o})$, in the region of $0 \leq \mathbf{r} \leq \mathbf{r}_\mathrm{o}$, instead of just one component of the velocity vector in a specific position $\mathbf{r} = \mathbf{r}_\mathrm{o}$. That is due to the two-dimensional characteristic of the electronic image sensor, which allows that a certain area of the fluid flow, instead of just one spatial position like in the traditional techniques, can be analyzed for a particular instant of time $t$ [12].

This two-dimensional characteristic of this measurement technique implies that robust signal processing techniques based on image processing should be adopted. Along the last years, this has required, and continues to require, hard work by researchers around the world. Basically, the research works in this field have been absorbed in developing new specific image processing techniques and new specific image processing algorithms for these ones, specific punctual improvements of old techniques and old algorithms, new specific equipments for instrumentation, and others. Although these works are very important in the scope of the velocimetry through image processing, they are just an item that should be analyzed (this is the reason by which it has been used the word specific in the last sentence) when it is desired to build an instrumentation system for the measurement of the velocity field of fluid flows using this kind of technique. This type of instrumentation system, involving its equipments and its algorithms, is named hereafter of Velocimetry System.

For the designing and implementation of an entire Velocimetry System, it is necessary and determinant first to establish its requirements and, after, to know all the existent and already developed algorithms and instrumentation equipments, to choose which of them will be used, and to know how to interconnect them. Finally, the resultant Velocimetry System from the procedure above must be checked to verify if it satisfies its initially stated requirements. If it is, the engineering work has been successfully done. If it is not, it should be considered or to improve the used algorithms and instrumentation equipments, or to choose other ones, and/or to develop new ones.

The purpose of the present article is to show the design and the implementation of image processing algorithms for the measurement of the two-dimensional velocity field of arbitrary fluid flows. For that, it has been necessary to develop a methodology for the conception and for the design of a Velocimetry System. In this methodology, the image processing algorithms are one part of many that compose an entire Velocimetry System. These image processing algorithms have been implemented in our software, whose name is IPVFlow, version V1.0 [12], which has been successfully applied by us in many mechanical systems in fluid dynamics, as fluid flows inside circular pipes [13] and fluid flows inside metallurgical ladles [6]. A detailed description about the architecture of this software can be found in the reference [14]. A description through block diagrams will be used along the current article, as a tool to explain the role and the functionality of the employed algorithms, always in the engineering point of view.

This article is organized in the following form: in section 2, the general principle of velocimetry is introduced and the implications of its application over fluid flows are described. With this, in this section, the methodology developed by us to the conception and to the design of a Velocimetry System is also presented. In section 3, the image processing algorithms are shown and explained in detail. Some necessary improvements of the image processing algorithms that exist in the literature are also shown. In section 4, it is discussed the results and the performance of the implemented algorithms for the image processing. For an illustrative purpose, frames previously captured from the traditional fluid flow inside a circular pipe have been used. In this section, a brief commentary about the uncertainty of the implemented algorithms is also established. In section 5, the conclusion of this article and the perspectives for future works will be discussed.

## 2 – THE PRINCIPLE OF A VELOCIMETRY SYSTEM

Generically, the principle of a Velocimetry System, when applied to fluid dynamics, consists in determining the distance covered by one and/or by an ensemble of particles on a well defined interval of time. With this objective, some micrometric particles are spread in the fluid flow. These particles are assumed small enough and with the same density of the fluid, so that, respectively, the drag force and the buoyancy force can be neglected. Also, these particles perfectly follow the streamlines of the fluid flow, implying that the lift forces are ignorable. Synthetically, it

can be supposed that the particles do not interfere in the fluid flow, acting simply as a tracer [12]. The way as the particle displacement is measured determines the type of instrumentation technique should be adopted. In the present case it is employed by us image instrumentation techniques and so, the Velocimetry System is through image processing.

To capture the information from the fluid flow, the tracer particles are illuminated by a coherent light source (usually a laser) and its images are captured by a camera with an electronic image sensor (usually a CCD but most frequently now a CMOS). The camera captures successive frames of the particle ensemble trajectory with a stable time-base $\Delta t$. The frequency with which the frames are captured from the fluid flow is known as frame rate, represented here by $T_q$.

An example of a typical instrumentation system employed for the measurement of velocity fields of fluid flows is shown in Figure 1. It is composed by a laser source, optical lens, tracer particles, electronic circuits for triggering the equipments, a CCD camera, and a Personal Computer (PC). The trigger device has been used to synchronize the laser source with the CCD camera for the frame acquisition. Also, this equipment has a relevant function in periodic fluid flows or in fluid flows initiated by an external event [12].

It is important to notice that each frame represents the spatial behavior of the fluid flow in a particular instant of time, while the sequence of frames provides the information about the fluid dynamics. Then, the spatial structures of the fluid flows can be calculated and evaluated as time evolves.

In this sense, the image processing techniques provides a three-dimensional measurement, two of these dimensions are spatial and one of these dimensions is temporal. For the same optical devices, the spatial and temporal resolutions are directly related with the electronic image sensor characteristics. In a simple way, how much larger the pixel density in the CCD sensor, more spatial resolution will have the measurement. In the same way, how much higher the frame rate $T_q$, more temporal resolution the measurement will have.

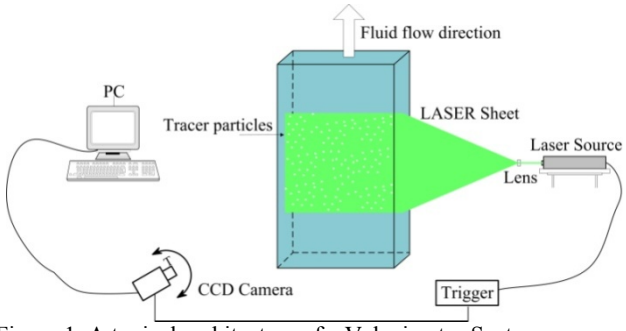


Figure 1. A typical architecture of a Velocimetry System.

Analyzing the experimental apparatus of the Figure 1, which is applied over an arbitrary fluid flow, it can be seen that a Velocimetry System can be segmented in two functionally distinct subsystems, named here of the image formation subsystem (IFS) and the image processing subsystem (IPS). The task of IFS is to form and to capture the images from the fluid flow. This subsystem is composed by the tracer particles, the laser source, trigger circuits for synchronization, optical lens, and a camera with an electronic image sensor. In resume, the subsystem IFS just involves the equipments used in the instrumentation. On the other hand, the IPS subsystem just comprises the PC, where the frames captured from the fluid flow are stored for future analysis by the image processing algorithms. These subsystems are shown schematically in the Figure 2.

However, each one of the IFS equipments must be configured for the correct capture and the correct formation of the frame. Usually, in less automated systems, its configuration is done by the experimenter, who, for example, determines the increase of the laser intensity and/or the shutter time of the camera when he verifies that the image sent to the IPS does not have enough bright and contrast. There is a feedback in this process: the equipments must be continuously regulated by the analysis of the captured frames. This action of the IPS on the IFS is symbolized in Figure 2 through a control signal $S_c(t)$.

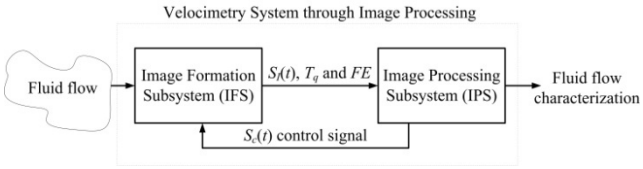


Figure 2. A Velocimetry System through Image processing.

The image signal $S_I(t)$ output by the camera, the camera frame rate $T_q$ and the scale factor $FE$ are sent to IPS. The scale factor $FE$ relates the coordinates of the particle ensemble (object domain, perspective, or scene) with the coordinates of its images (image domain, projection, or image) [15]. The image signal $S_I(t)$ and the parameters $T_q$ and $FE$ are used in the IPS by its image processing algorithms for the calculation of the velocity field [12].

It should be noted that the unique information that the IPS needs is the image signal $S_I(t)$ and the parameters $T_q$ and $FE$, which completely characterize the fluid flow and the IFS subsystem, respectively. That is, for the IPS, it is not important the nature of the physical system, not even which is the equipments employed in the IFS, but just the knowledge of the 3 previous commented quantities: $S_I(t)$, $T_q$, and $FE$. Therewith, it is possible to compute the velocity field using the developed algorithms.

The abstraction level that has been used here to describe the Velocimetry System (through just 2 subsystems) is important, because it propitiates that algorithms employed in IPS can be changed, can be improved or can be developed, independently of the type of fluid flow in which these algorithms are applied and of the type of equipments employed in the IFS subsystem. This methodology is essentially also important when the objective is to implement a Velocimetry System for engineering purposes.

Considering the information above as a basis for the development of a Velocimetry System, in the remaining paragraphs of this section, the principle of velocimetry

applied to fluid flows will be dealt. The Figure 3 illustrates the situation where a particle ensemble describes an arbitrary trajectory in a fluid flow. The ensemble of particles passes by the arbitrary points $\boldsymbol{P_0}$, $\boldsymbol{P_1}$ and $\boldsymbol{P_2}$ in also arbitrary times given by $t_0$, $t_1$ and $t_2$, respectively. Considering $\Delta t_j \approx constant = \Delta t$, the time-mean velocity vector of this particle ensemble for an amount of time $J \cdot \Delta t$ is given by the following equation:

$$\langle \mathbf{v} \rangle_o = \frac{\sum_{j=1}^{J} \Delta \mathbf{r}_j}{\sum_{j=1}^{J} \Delta t_j} = \frac{1}{J} \cdot \sum_{j=1}^{J} \mathbf{v}_j \qquad (1)$$

where $j$ is the time index, $\mathbf{r} = x\mathbf{e}_x + y\mathbf{e}_y + z\mathbf{e}_z$, $(\mathbf{e}_x, \mathbf{e}_y, \mathbf{e}_z)$ are respectively the unitary vectors in the $(x, y, z)$ directions, the angle brackets denote the time-mean operator, and the subscript "$o$" denotes the velocity of the object, in this case, the particle ensemble. For $j = 1$, the equation (1) furnishes the instantaneous velocity vector of the particle ensemble.

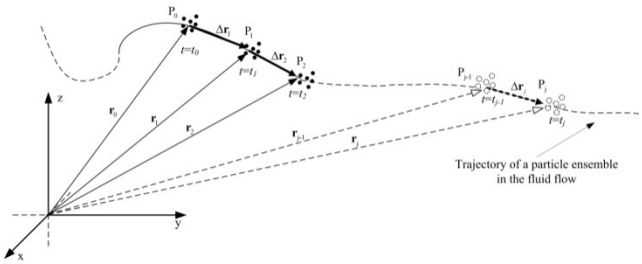


Figure 3. An arbitrary trajectory of a particle ensemble in a fluid flow.

The time base $\Delta t$ is related directly to the camera frame rate $T_q$. Thereby:

$$\Delta t = 1/T_q \qquad (2)$$

where the camera frame rate $T_q$ has physical dimension of $[T_q] = 1/s$.

The transformation of a perspective in a projection is a nonlinear operation where one of the spatial dimensions is eliminated. When the interest falls in dynamical quantities like the velocity, it is observed mathematically that there is some influences of this eliminated velocity component in the computation of the other ones. In certain situations, these influences may be neglected and this transformation becomes linear. Then, the object velocity vector can be obtained from the image velocity by just the multiplication of the constant $FE$ [12]. In these circumstances, for the time-mean velocity vectors:

$$\langle \mathbf{v} \rangle_o \approx FE \cdot \langle \mathbf{v} \rangle_i = FE \cdot T_q \cdot \sum_{\alpha=\{x,y,z\}} \langle \Delta r_\alpha \rangle_i \mathbf{e}_\alpha \qquad (3)$$

where $\langle \Delta \mathbf{r} \rangle_i$ is the time-mean vectorial displacement of the particle ensemble in the frames captured along the time, $T_q$ is the camera frame rate, $FE$ is the scale factor that characterizes the IFS subsystem and $\alpha$ is just a index that can assume $x$, $y$, or $z$ and indicates each direction of the particle ensemble displacement.

The correct adjustment of the time base directly depends on the time scales that the physical quantities of the fluid flow change. Therefore, it is an excellent approximation the situation where the time interval $\Delta t$ is smaller than the time scales of the fluid flow. For turbulent regimes, considering the time scale of the large structures of the turbulence [16] and the Nyquist criterion [17] for the reconstruction of the image signal, the $\Delta t$ time must satisfy [13]:

$$\Delta t \leq L_c/(2 \cdot U_c) \qquad (4)$$

where $L_c$ is the characteristic length and $U_c$ is the characteristic velocity of the fluid flow under analysis.

The algorithms that compose the subsystem IPS can be divided by its functionality in the form that it is shown in the Figure 4. The analog signal $S_I(t)$ originating from the IFS subsystem is transformed into bitmap frames through a frame grabber. These captured frames, in general, should be pre-processed and its result is represented here by $\{Q_j\ Q_{j-1}\ Q_{j-2} \ldots Q_0\}$. The frames $Q_j$ has size of $n_l\ x\ n_c$ pixels, where $n_l$ is the number of pixel lines and $n_c$ is the number of pixel columns of the camera image sensor. The pre-processing algorithms consist of noise filters, image segmentation, image enhancement, image restoration, and others [12][18][15]. After that, the frame sequence is applied to the processing algorithms that will calculate the velocity field. Finally, the post-processing algorithms are executed for the validation of the entire velocity field and to compute physical quantities of the fluid flow like vorticity, intensity of turbulence, circulation, and others [12].

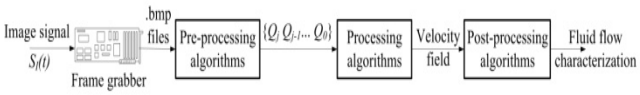


Figure 4 – The image processing subsystem (IPS).

In this work, due to the innumerous functional blocks involved in the overall Velocimetry System through image processing and to the impossibility to describe all of them in a single article, just the processing algorithms of the IPS subsystem will be presented. The pre-processing and post-processing algorithms will be a subject of future publications.

## 3 – THE PROCESSING ALGORITHMS

The algorithms employed in the processing stage are shown in Figure 5. It has been decided by us to employ the cross-correlation technique for the calculation of the particle ensemble displacement [19]. This technique is useful if one of the measurement requirements is the spatial resolution. Succinctly, the processing stage is composed by 3 blocks of image processing algorithms that calculate the cross-correlation between images selected in 2 different frames, that detect the cross-correlation peak

originated in this calculation, and that compute the velocity field.

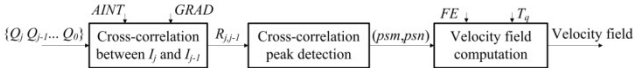


Figure 5. Image processing algorithms for the $Q_j$ frames.

First, the sequence of frames $\{Q_j\ Q_{j-1}\ Q_{j-2} \ldots Q_0\}$ coming from the pre-processing block, which has been commented in the penultimate paragraph of section 2, is grouped in pairs. Each pair of $\{Q_j, Q_{j-1}\}$ frames captured from the fluid flow produces a velocity field $\mathbf{v}_j$. Assuming that $j = \{1, 2, 3, \ldots, J\}$ frames are captured from the fluid flow, then $J - 1$ velocity fields can be obtained from this data. This process is named by us of frame grouping and is schematically shown in the Figure 6.

To compute each velocity vector that composes the velocity field $\mathbf{v}_j$, each pair of $\{Q_j, Q_{j-1}\}$ frames is subdivided into images with the same size, which is named respectively of $I_{j-1}$, for the images selected in the frame $Q_{j-1}$, and $I_j$, for the images selected in the frame $Q_j$. Each pair of $I_{j-1}$ and $I_j$ images will produce one velocity vector in a specific spatial position of the fluid flow and in a specific instant of time of its dynamics given by $t_j = j \cdot \Delta t$. The set of images $\{I_{j-1}, I_j\}$ that is selected in the frames $Q_j$ and $Q_{j-1}$ will allow to calculate all the velocity vectors that compose the entire velocity field $\mathbf{v}_j$ for this time of $t_j = j \cdot \Delta t$.

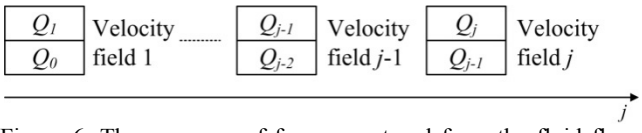


Figure 6. The sequence of frames captured from the fluid flow and its grouping to produce the velocity fields.

Each one of these pairs of $I_{j-1}$ and $I_j$ images are then cross-correlated and its result is another image, here denoted by $R_{j,j-1}$. The particle ensemble inside the $I_{j-1}$ and $I_j$ images can be interpreted as a "particle pattern" of a specific region analyzed in the fluid flow [12]. This particle pattern must remain almost invariant in the instants of time indexed by $j - 1$ and $j$. In this way, it can be assured that there will be correlation between the $I_{j-1}$ and $I_j$ images, which strictly means that an $R_{j,j-1}$ image with a well defined peak is produced. This cross-correlation peak has to be detected and its coordinate $(psm, psn)$ has to be sent to the next block of the processing stage for the velocity vector calculation. The selection procedure of the $I_{j-1}$ and $I_j$ images and its correlation scheme are shown in Figure 7.

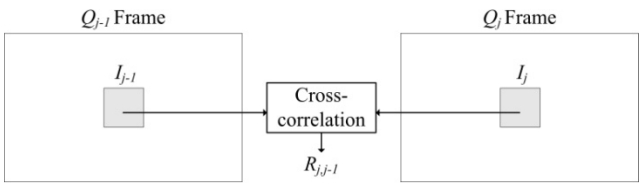


Figure 7. $I_{j-1}$ and $I_j$ images selection and its correlation for the velocity vector calculation.

The size of the $I_{j-1}$ and $I_j$ images depends on the number of particles that there are within them. Usually, at least 3 particles have been shown to be enough for an acceptable correlation in the experiments carried out by us [12]. As a direct consequence, the magnification of optical instruments, the particles density in the fluid flow, and the diameter of the particles employed in the experiment will determine the minimal size of the $I_{j-1}$ and $I_j$ images that could be selected respectively in the $Q_{j-1}$ and $Q_j$ frames. How much smaller are the selected images, more velocity vectors can be calculated from the same $Q_{j-1}$ and $Q_j$ frames, increasing its density and consequently improving the description of the fluid flow by an increment of the spatial resolution of the measurement.

In the next subsections 3.1, 3.2, and 3.3 the algorithms that compose the processing stage will be individually described. The sequence of frames $\{Q_j\ Q_{j-1}\ Q_{j-2} \ldots Q_0\}$ used here for the exemplification of the implemented algorithms has been extracted from a fluid flow inside a circular pipe [13], a typical geometry very explored in the literature [2][9] and useful here to compare with our results and to validate the image processing algorithms developed by us. Note that the frames that will be presented in the next subsections have already been pre-processed by the algorithms of the subsystem IPS shown in Figure 4.

### *3.1 The cross-correlation between $I_{j-1}$ and $I_j$ block*

The $I_{j-1}$ images selected in the $Q_{j-1}$ frame receive in this image processing block the name of interest areas. In the same way, the $I_j$ images selected in the $Q_j$ frame receive the name of search areas [12].

The shape of the interest and the shape of the search areas can assume many types [20]. Depending of the fluid flow, a specific shape can be more suitable because it can decrease the uncertainty in the measured velocity vector. However, how much more complicated is the shape chosen, more complicated will be the algorithms and more processing time will be required for its selection and its correlation [12]. In this work, for simplicity, the shape of the interest and search areas selected in the frames is square.

The size of the interest and search areas is a parameter that must be chosen by the experimenter. This parameter should be specified after a simple visual inspection of the captured frames and after a few tries executing the developed algorithms. This parameter is represented in our algorithms by *AINT*. Each one of the areas of interest selected in the frame $Q_j$ is specified by its discrete coordinates $(l, c)$. The coordinate pair $(l, c)$ can assume any value in the intervals of $0 < l < L$ and $0 < c < C$. In the present case, considering the fact of our interest and search areas to be square, the maximum value that $L$ and $C$ can assume is $AINT$. In the Figure 8a, it is shown a frame $Q_j$ captured from the fluid flow and its subdivision in $I_j$ images with size of $AINT$=80 pixels.

To improve the spatial resolution of the measurement, it has been adopted by us an overlapping technique that has

been already used by researchers in the pre-processing of speech signals [21]. The pixel distance between 2 consecutively selected areas of interest is determined by the variable $GRAD$. This variable is also specified and should be tested by the experimenter in the same way explained for $AINT$. If it is considered the case of $GRAD < AINT$, there will be an overlapping between two consecutively selected areas of interest. That is, there will be particles that will pertain to two or more neighbor areas of interest. This technique provides an improvement of the velocity vector density in relation to the traditional case, which is without overlapping. This procedure is graphically shown in Figure 8b.

The next step is to cross-correlate the $I_{j-1}$ and $I_j$ images that have been previously selected in the $Q_{j-1}$ and $Q_j$ frames. Mathematically, considering a coordinate system located at the geometric center of the interest and search areas, this means:

$$R_{j,j-1}(m,n) = \sum_{l=-\frac{AINT}{2}}^{\frac{AINT}{2}} \sum_{c=-\frac{AINT}{2}}^{\frac{AINT}{2}} I_{j-1}(l,c) \cdot I_j(l+m, c+n) \quad (5)$$

where $(l,c)$ are the $I_{j-1}$ and $I_j$ image coordinates in pixel units, and $(m,n)$ are the coordinates of the correlation space $R_{j,j-1}$, also in pixel units.

The result of the cross-correlation between the interest areas and the search areas is shown in the Figure 9. In this case, the images sizes have been set to $AINT$=80 pixels. These images have been padded with zeros until its size reached the double of its original dimensions, that is, $2xAINT$. The most intense peak in the image $R_{j,j-1}(m,n)$ that appears in this figure corresponds to the point where there is the better correlation between the particle patterns in the $I_{j-1}(l,c)$ and $I_j(l,c)$ images. This information is crucial for the velocity vector calculation. The offset of the $R_{j,j-1}$ has been subtracted.

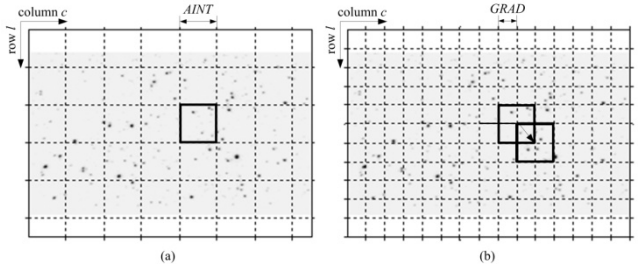


Figure 8. (a) The frame $Q_j$ and its $I_j$ images, (b) The overlapping in the selected areas of interest.

The surface graph of the image $R_{j,j-1}(m,n)$ is presented in Figure 10a. It can be observed clearly in this figure that there is a peak with large amplitude when compared with the others ones. This peak is the same that such most intense peak that has been observed in the Figure 9.

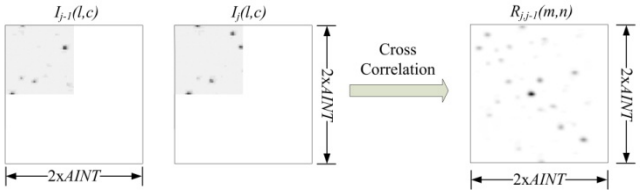


Figure 9. The $R_{j,j-1}$ resultant image from the cross-correlation between $I_{j-1}$ and $I_j$.

The other peaks can be interpreted as an inherent noise to the measurement process. This noise permeates all the fluid flow under analysis and appears in the cross-correlation image $R_{j,j-1}(m,n)$ as false correlation peaks. How much more intense are these peaks, more the measurement is affected by the noise. Large differences between the most intense peak and the other ones in the cross-correlation space indicate that the calculated velocity vector may be considered as a real measurement of the fluid flow. The ratio between the two more intense peaks of the cross-correlation space can be used for the estimation of the signal to noise ratio of the measurement. With this, it is possible to develop a filter to be used for validation of the calculated velocity vectors in the post-processing stage [12].

### *3.2 The cross-correlation peak detection block*

As commented earlier, after the calculation of the $R_{j,j-1}(m,n)$ image, it must be determined which is the most intense peak and which is its coordinates in the correlation space. These coordinates will supply the information about the displacement of the particle ensemble between two successive instants of time indexed by $j-1$ and $j$.

The coordinates of the cross-correlation peak are computed through an algorithm expressed by this equation:

$$(pm, pn) = \max\{R_{j,j-1}(m,n)\} \quad (6)$$

in which $(pm, pn)$ are the coordinates of the most intense peak of $R_{j,j-1}(m,n)$ detected by the algorithm that implements the function max{}. For the example case of Figure 9, the computed coordinates are $(pm, pn)$=(80,72) pixels, which means no vertical but just horizontal displacement.

However, these coordinates correspond to a first approximation of the real cross-correlation peak. Due to the quantization done by the electronic image sensor to the real image, the most intense peak in the correlation space of image $R_{j,j-1}(m,n)$ does not correspond necessarily to the real most intense peak. One better approximation for the location of the maximum correlation peak can be obtained if it is also considered in the analysis its neighbor pixels. In this way, a sub-pixel approximation of its location can be done. This sub-pixel approach provides better precision in the displacement estimation of the particle pattern as well as better precision in the computation of the velocity vector. Then, it becomes important to understand how the particles scatter the incident light originated by the laser source. This is a not

trivial problem since the used particles in general have an irregular shape [22].

Considering a coherent laser source with its confocal cavity perfectly adjusted to the first resonant mode, it can be assumed that the transversal section of its beam will be a Gaussian function of the spatial coordinates. If the particles diameters are big enough such that the diffraction effects are worthless, it is possible to assume that the cross-correlation peak of Figure 10a also has a Gaussian shape in relation to its spatial coordinates [12].

Then, it is possible to fit an analytical Gaussian function for the correlation peak of Figure 10. With that, the coordinates of the real cross-correlation peak can be calculated with a better precision. This procedure corresponds to a second approximation in relation to the previous method, which has considered only the coordinates of the peak with more intensity in the correlation space. With this strategy, it can be find the real coordinates with a resolution of 1/10 to 1/20 pixels. A deep discussion about this subject is found in reference [12].

The Gaussian fit implemented by us considers only the 4 neighbor pixels of the pixel with more intensity $(pm, pn)$. The Figure 10b illustrates this scheme. This Gaussian fit is applied in each coordinate of the pair $(pm, pn)$, generating new coordinates named here by $(psm, psn)$. The coordinate $psm$ is obtained using the pixels $pm \pm 1$ while the coordinate $psn$ is obtained by the pixels $pn \pm 1$. The equations that determine these new coordinates are expressed by [23]:

$$psm = pm + c(\varsigma = pm)$$
$$psn = pn + c(\varsigma = pn) \tag{7}$$

in which

$$c(\varsigma) = \frac{lnR_{j,j-1}(\varsigma - 1) - lnR_{j,j-1}(\varsigma + 1)}{2lnR_{j,j-1}(\varsigma - 1) - 4lnR_{j,j-1}(\varsigma) + 2lnR_{j,j-1}(\varsigma + 1)}$$

This cross-correlation peak correction algorithm has been applied to the $R_{j,j-1}$ image of the Figure 10a resulting in new coordinates given by $(psm, psn)$=(80.1386, 71.7656) pixels.

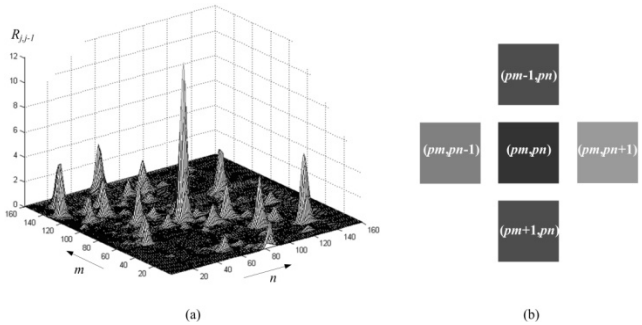


Figure 10. (a) Surface graph of the $R_{j,j-1}$ image, (b) A Gaussian fit for the correlation peak.

### *3.3 The velocity field computation block*

With the coordinates of the most intense peak of $R_{j,j-1}$ computed, corrected by the subpixel algorithm, and then given by $(psm, psn)$, the next task is to determine the velocity vector of the correspondent particle ensemble. Considering $j$=1 and the criteria established by the equation (4), it is easy to see that the equation (3) provides the instantaneous velocity vector for the particle ensemble within the $I_{j-1}$ and $I_j$ images. In this way, it is possible to write:

$$\mathbf{v}_o \approx FE \cdot \Delta\mathbf{r}_i \cdot T_q \tag{8}$$

The vector displacement $\Delta\mathbf{r}_i$ of the particle ensemble inside the interest area is calculated by the difference between the calculated $(psm, psn)$ coordinates and the coordinates that locates the center of the image originated by the cross-correlation $R_{j,j-1}$, given by $(AINT, AINT)$. Mathematically, for the two-dimensional case:

$$\Delta\mathbf{r}_i \approx (AINT - psn)\mathbf{e}_x + (AINT - psm)\mathbf{e}_y \tag{9}$$

Until now, it has been exposed how to obtain the velocity vector for a specific time $t_j = j \cdot \Delta t$ and a specific spatial coordinate $(l, c)$ of the frames captured from the fluid flow. For the measurement of the whole instantaneous velocity field, it is just necessary to apply the same procedure presented in the last sections to the remainder areas of interest and search areas that compose the frames. In resume, the whole instantaneous velocity field is obtained by the calculation of all velocity vectors of all the $I_{j-1}$ interest areas and the $I_j$ search areas selected respectively from the $Q_{j-1}$ and $Q_j$ frames, defined by a size of $AINT$ pixels and an overlapping of $GRAD$ pixels.

The time evolution of the velocity field is determined by the processing of the $\{Q_j\ Q_{j-1}\ Q_{j-2} \ldots Q_0\}$ sequence of frames, which has been captured from the fluid flow in the time indexed by $j = \{1, 2, 3, \ldots, J\}$ or in other words, in the time given by $t = \{1/T_q, 2/T_q, 3/T_q, \ldots, J/T_q\}$. With that, time-mean quantities as well the dynamics of spatial quantities of the velocity field can be computed and analyzed.

## 4 – DISCUSSION AND RESULTS

The Figure 11 shows 2 successive frames captured from the fluid flow internal to a circular pipe with spatial and temporal average velocity of 0.53 m/s. The camera frame rate has been $T_q$=500F/s. The frames have the size of 624x470 pixels and have been subdivided in interest and search areas of *AINT*=80 pixels, with an overlapping of $GRAD$=40 pixels. The value of the scale factor in this case is $FE$=1.442307·10$^{-4}$ m/pixel. The Processing algorithms discussed in the section 3 have been implemented in the MATLAB environment.

The selection of the previously commented $I_{j-1}$ and $I_j$ images also can be observed in Figure 11. For a time indexed by $j-1$, internally to the $I_{j-1}$ area of interest, it is possible to verify the pattern formed by the particles spread in the fluid flow. In the following instant of time indexed by $j$, in the $I_j$ search area, it can be observed the same particle pattern of the previous area of interest. This particle pattern is almost unchanged and has just a small displacement to the right. It is this displacement that is

measured when equation (9) is applied. Note that there is some difference in the intensity of the particle images during its motion from the $I_{j-1}$ image to the $I_j$ image. It is due to the transversal motion executed by the particles in relation to the frame plane. In this case, this movement is not critical, because the particles continue to remain in the frame plane.

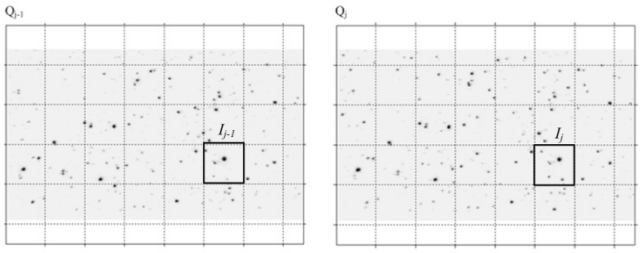


Figure 11. The $Q_{j-1}$ and $Q_j$ frames for a fluid flow internal to a circular pipe.

The Figure 12a shows the instantaneous velocity field computed for the $Q_{j-1}$ and $Q_j$ frames of Figure 11. This velocity field has been obtained by the image processing algorithms described in the section 2 of this work. The plotted velocity vectors are in scale. The presence of spurious vectors can be observed in Figure 12a, where some of them have been circulated to stand out against the correct ones. Such erroneous vectors are resultant from the incorrect determination of the correlation peak.

In some cases, a real correlation peak does not exist. Then, the low intensity peaks that appear in the correlation space $R_{j,j-1}(m,n)$ are derived from the noise that affects the measure. This occurs by the absence or the insufficient presence of particles in the interest area and, as a consequence, in the search area. This problem can be solved increasing the amount of the spread particles and/or increasing the value of the variable $AINT$. In the Figure 12a it can be observed that the spurious vectors correspond to the regions of the frames $Q_{j-1}$ and $Q_j$ of Figure 11 where the particle density is too small. In other cases, as previously commented, the component of the velocity vector transversal to the captured frames influences and degenerates the particle pattern in successive times indexed by $j-1$ and $j$. Then, the area of interest $I_{j-1}$ becomes substantially different of the search area $I_j$, not being more possible to obtain satisfactory correlation between both. An intuitive solution is to increase the camera frame rate $T_q$. However, considering that the turbulence influences the fluid flow in an unexpected way in the space and in the time, it will never be possible to determine a frame rate $T_q$ that is valid for the entire spatial region and for the entire time interval of the analyzed fluid flow.

This means that the post-processing algorithms shown in Figure 4 become essential to validate the instantaneous velocity field obtained in the image processing block. In general, the spurious vectors have magnitude and direction very different of the correct ones. Thus, these spurious vectors can be eliminated with a simple filter or with some statistical algorithm. Afterwards, these eliminated vectors can be replaced by others that are obtained by an interpolation algorithm, which uses a linear combination of the velocity vectors neighbor to the eliminated ones to generate another. These new vectors constitute a well approximation to the real measurement [12].

However, in many applications, the interest falls only in the time-mean velocity field of the fluid flow. In these cases, assuming that the spurious vectors are randomically distributed in the processed frames, its influence on the final time-mean velocity field is small. These influences will be smaller how much more frames $Q_j$ are used for the calculation of the time-mean velocity field.

The Figure 12b shows the time-mean velocity field for $J$=100 frames captured from a fluid flow internal to a circular pipe. The time-mean velocity field has been obtained using the methodology of the section 2 and using the equation (1) for each instantaneous velocity field measured from the fluid flow. Qualitatively, it can be observed that the spurious vectors that appear in the instantaneous velocity field of Figure 12a naturally disappear in the time-mean velocity field of the Figure 12b. Due to the smaller magnitude range of the velocity vectors, the presentation and the visualization of the velocity field also becomes better.

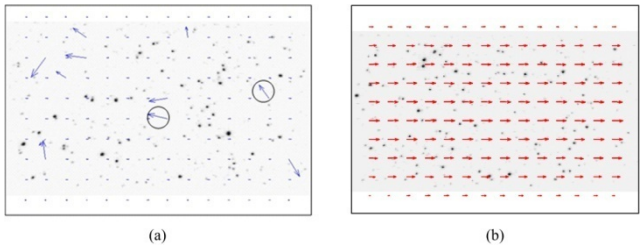


Figure 12. (a) The instantaneous velocity field, (b) The mean velocity field for $J$=100 frames.

Quantitatively, on the other hand, if the spurious vectors are not eliminated, there will be an increment of the uncertainty in the measurement. Due to the random characteristic of the turbulence, as it has been previously commented, if more $Q_j$ frames are used, smaller will be its influence in the measurement. In many cases, depending on the number of frames that is used in the time-mean process, the uncertainties in the time-mean velocity fields can be tolerable and therefore it is not necessary to post-process the instantaneous velocity fields. The main advantage in this is the time efficiency, since usually it is necessary to process thousands of frames and the post-processing algorithms are time-consuming.

## 5 – CONCLUSIONS

Although the physical basis of the techniques for the measurement of velocity fields by image processing is well-known by many researchers around the world, its using is already restricted to a few laboratories. Almost all research works in this prominent area is just focused in developing new specific image processing algorithms and instrumentation equipments or in improving these ones. Research works that consider the engineering aspects involved in the conception and in the design of the entire

Velocimetry System are still rare. The result is that a few companies develop and offer this type of instrumentation system in the market with higher costs, inhibiting its complete dissemination and its broad use by the researchers.

In fluid dynamics, the velocimetry techniques through image processing became a powerful tool because the two-dimensional characteristic of the electronic image sensor allows the measurement of a whole velocity field instead of just one velocity vector for a given time. Also, the large density of pixels as well as the higher frame rates of the current electronic image sensors propitiates the measurement of velocity fields with high spatial and temporal resolution, respectively.

For this purpose, in this work it has been introduced by us a methodology for the conception and the design of a Velocimetry System through image processing, applied to fluid flows. For that, the Velocimetry System has been subdivided in two functionality distinct subsystems, named here by IFS and IPS. This methodology has been used by us with success to the development of new or to the improvement of our image processing algorithms. It has been also important in discussions done with researchers from other areas of the knowledge like computer scientists and physicists. All of this has propitiated the application of our Velocimetry System in different types of fluid flows. Also, this methodology seems to be useful for researchers interested just in the application or interested just in the development of a Velocimetry System.

A Velocimetry System through image processing is complex because involves physical concepts about fluid dynamics, instrumentation techniques and theory of signal processing. In this way, considering the impossibility of describing all the system in a single article, in this work it has been just presented by us the algorithms for the Processing block, one of the algorithm blocks that compose the IPS.

The implemented cross-correlation algorithm presented a fine performance. The shape of the interest and search areas chosen here has been shown to be adequate for many types of fluid flows in which it has been applied by us. The implementation of a Gaussian fit for the determination of the correlation peak made the measurement process to be more accurate and thus, to have a better agreement with the real fluid flow.

Some spurious velocity vectors had appeared in the use of the developed algorithms. These are inherent to the measurement process and it is due to the unpredictable behavior of the turbulence, which is a consequence of the nonlinear aspects of the systems in fluid dynamics. To solve this problem, it is necessary to apply post-processing algorithms to validate the obtained velocity field or to improve the density of tracer particles in the captured frames.

To conclude, the algorithms presented satisfactory results with an uncertain in the measured velocity vectors less than 1.6%. For the frames captured from the fluid flow inside a circular pipe, that has been presented here for demonstration of our image processing algorithms, the computation of the instantaneous velocity field takes around 7.6s while the time-mean velocity field for $J$=100 frames takes around 966s.

## ACKNOWLEDGEMENTS

The author Roger Pizzato Nunes acknowledges the financial support that he has received from CNPq, Brazil.

## REFERENCES

[1] Landau, L.D., and Lifshitz, E.M., "Fluid Mechanics", Course of Theoretical Physics, Vol. 6, Addison-Wesley, London, England, 1959.

[2] Schlichting, H., and Gersten, K., "Boundary-Layer Theory", Springer-Verlag, Berlin, Germany, 2000.

[3] Yildirim, I., Cetiner, O., and Unal, M.F., "PIV Measurements of the wake interactions for a Circular Cylinder behind an Airfoil", Proceedings of the 6th International Symposium on Particle Image Velocimetry, Pasadena, USA, 2005.

[4] Chow, Y.C., Katz, J., Uzol, O., and Meneveau, C., "An Investigation of Axial Turbomachinery Flows Using PIV in an Optically-Unobstructed Facility", Proceedings of the 9th International Symposium on Transport Phenomena and Dynamics of Rotating Machinery, Honolulu, Hawaii, 2002.

[5] Vieira, E.D.R., Dall'Agnol, E., Mansur, S.S., Mazza, R.A., Pinotti, M., and Braile, D.M., "Flow visualization of heart valves prostheses in a steady flow model", Revista Brasileira de Engenharia Biomédica, vol. 15, no. 1-2, pp. 63-68, 1999.

[6] Nunes, R.P., Pereira, J.A.M., Vilela, A.C.F., and van der Laan, F.T., "Visualization and analysis of the fluid flow structure inside an elliptical steelmaking ladle through image processing techniques", Journal of Engineering Science and Technology, vol. 2, no. 2, pp. 139-150, 2007.

[7] Gioia, G., and Chakraborty, O., "Turbulent Friction in Rough Pipes and the Energy Spectrum of the Phenomenological Theory", Physical Review Letters, vol. 96, no. 4, pp. 1-4, 2006.

[8] Goldenfeld, N., "Roughness-Induced Critical Phenomena in a Turbulent Flow", Physical Review Letters, vol. 96, no. 4, pp. 1-4, 2006.

[9] Shames, I.H., "Mechanics of Fluids", McGraw-Hill, New York, USA, 1992.

[10] Doebelin, E.O., "Measurement Systems Application and Design", McGraw-Hill, New York. USA, 1990.

[11] Lai, W.T., Bjorkquist, D.C., Abbott, M..P., and Naqwi, A.A., "Video systems for PIV recording", Journal of Measurement Science and Technology, vol. 9, no. 3, pp. 297-308, 1998.

[12] Nunes, R.P., "Design and implementation of an electro-electronic instrumentation system for flow characterization through digital image processing", Master of Science Dissertation, Universidade Federal do Rio Grande do Sul, RS, Brasil, 2005.

[13] Nunes, R.P., and van der Laan, F.T., "Velocity field measurement for a high turbulent duct flow through digital image processing", Proceedings of the 11th Brazilian Congress of Thermal Sciences and Engineering, December 5-8, Curitiba, Brasil, 2006.

[14] Nunes, R.P., and van der Laan, F.T., "Design of a software architecture for Velocimetry Systems", Journal of Computer Science, vol. 6, no. 3, pp. 56-65, 2007.

[15] Schalkoff, R.J., "Digital Image Processing and Computer Vision", John Wiley & Sons, Canada, 1989.

[16] Freire, A.P.S., Menut, P.P.M., and Su, J., "Turbulência", Associação Brasileira de Ciências Mecânicas (ABCM), Rio de Janeiro, Brasil, 2002.

[17] Oppenheim, A.V., and Schafer, R.W., "Discrete-Time Signal Processing", Prentice-Hall, New Jersey, USA, 1989.
[18] Gonzalez, R.C., and Woods, R.E., "Processamento de Imagens Digitais", Edgard Blücher, São Paulo, Brasil, 2002.
[19] Adrian, R.J., "Particle-imaging techniques for experimental fluid mechanics", Annual Reviews in Fluid Mechanics, vol. 1, no. 23, pp. 261-304, 1991.
[20] Belmont, M.R., and Jardon, S.P.V., "Generalized cross-correlation functions for engineering applications. Application to experimental data", Experiment in Fluids, vol. 29, no. 5, pp 461-467, 2000.
[21] Nunes, R.P, Gómez, J.C., and Barone, D.A.C., "FPGA Hardware for Speech Recognition Using Hidden Markov Models", Proceedings of the International Conference on Spoken Language Processing, Denver, USA, pp. 2541-2544, 2002.
[22] van de Hulst, H.C., "Light scattering by small particles", John Wiley & Sons, New York, USA, 1957.
[23] Nobach, H., and Honkanen, M., "Two-dimensional Gaussian regression for sub-pixel displacement estimation in particle image velocimetry or particle position estimation in particle tracking velocimetry", Experiments in Fluids, vol. 38, no. 4, pp. 511-515, 2005.

## BIOGRAPHIC DATA

Roger Pizzato Nunes was born in Porto Alegre, RS, Brasil on August 11, 1981. He received his B.Sc. degree in Electrical Engineering and his B.Sc. degree in Physics from the Universidade Federal do Rio Grande do Sul (UFRGS) in, respectively, 2003 and 2005. He also received his M.Sc. degree in Mechanical Engineering from the same above commented University in 2005. Since 2005, he has been a Ph.D. candidate in Sciences at the Institute of Physics of the same previous commented University. His research areas of interest resides on signal processing, fluid dynamics, and plasma physics.